JOURNAL OF MATERIALS SCIENCE 29 (1994) 1595–1600

Effect of grain boundary phase on the thermal conductivity of aluminium nitride ceramics

CHING-FONG CHEN*, M. E. PERISSE‡, A. F. RAMIREZ§
Keramont Corporation, Tucson, AZ 85714, USA
N. P. PADTURE¶, H. M. CHAN
Lehigh University, Bethlehem, PA 18015, USA

AlN with high thermal conductivity was fabricated by pressureless sintering with Y_2O_3 as the sintering aid. The thermal conductivity was observed to increase with sintering time (up to 8 h) at 1810 °C. The distribution of the sintering aid was identified as one of the major factors influencing the thermal conductivity in AlN. Non-uniform distribution of the grain boundary phase was found to be associated with a significant amount of porosity, resulting in the enhancement of phonon scattering and thereby lowering the thermal conductivity.

1. Introduction

With both the increasing density of semiconductor devices, and the increasing power from these devices, substrates having high thermal conductivities are needed [1–3]. Without efficient heat dissipation, the increased circuit operating temperatures would lead to increased device failure rates. Also, as the size of the silicon chip becomes larger, matching the thermal expansion coefficient of the substrate has become critical in minimizing thermal stresses and thermal fatigue [1–3].

All the materials currently being considered for substrate applications have limitations. The thermal conductivity of diamond is the highest among existing materials, but its application is limited due to its high cost. Silicon carbide (SiC) has high thermal conductivity, but it also exhibits a high dielectric constant and low electrical resistivity. Unfortunately, both the latter properties are in some cases undesirable for substrate materials. Although beryllium oxide (BeO) has both high thermal conductivity and electrical resistivity, its use as a substrate material is restricted because of its toxicity. The theoretical thermal conductivity of boron nitride (BN) is very high, but this value can only be achieved in fully dense high-purity material, which is difficult to process. Unfortunately low-density BN has a dramatically reduced thermal conductivity and mechanical strength, making it unacceptable for microelectronic applications.

Aluminium nitride (AlN) has emerged as a favourable candidate because of its high thermal conductivity, a thermal expansion coefficient which closely matches that of silicon, good electrical insulation and adequate mechanical properties [1–3]. Single-crystal AlN has a theoretical thermal conductivity of 320 $W m^{-1} K^{-1}$ [4–6]. However, due to the imperfections of polycrystalline structures, the thermal conductivity of polycrystalline AlN is always lower than the theoretical value. Several parameters have been identified as having an influence on the thermal conductivity of AlN ceramics [7–12]; these include impurity content, porosity, free oxygen content, amount and distribution of grain boundary phase, grain size, dislocation density, presence of antiphase boundaries etc. Since thermal conductivity is proportional to the mean free path of phonon transmission, defects can reduce the mean free path and thus reduce the thermal conductivity. Most of these defects are related to the grain boundary phase. The objective of the present work is thus to identify the role of the grain boundary phase in the thermal conductivity.

2. Experimental procedure

2.1. Sample preparation

An AlN raw powder synthesized by the carbothermal reduction nitridation method was used. The chemical and physical properties of the starting AlN powder are listed in Table I [13]. A composition containing 2.0 wt % of Y_2O_3 (Union Molycorp, White Plains, New York) was prepared. The starting powders were ball-milled in acetone with a dispersant for 2 h using AlN grinding media. Binder and plasticizer were premixed in acetone before adding to the slurry. The slurry was subsequently granulated in a spray-dryer. Green parts were uniaxially cold-pressed at 170 MPa into specimens 3 cm × 3 cm × 0.12 cm. Binder removal was carried out in a nitrogen environment, and was followed by sintering for varying times at 1810 °C in a graphite resistance furnace. A mild nitrogen gas flow

* *Present address*: LECO Corporation, Technical Ceramics Division, PO Box 211688, Augusta, GA 30917, USA.
‡ *Present address*: Saxonburg Ceramics Inc., Saxonburg, PA 16056, USA.
§ *Present address*: MER Corp., Tucson, AZ 85706, USA.
¶ *Present address*: NIST, Gaithersburg, MD 20899, USA.

0022–2461

TABLE I Chemical analysis and physical properties of as-received AlN powder

O (wt %)	C (p.p.m.)	Fe (p.p.m.)	Si (p.p.m.)	Mg (p.p.m.)	Tap density ($g\,cm^{-3}$)	Surface area ($m^2\,g^{-1}$)	D_{10} (μm)	D_{50} (μm)	D_{90} (μm)
1.39	350	20	40	20	0.65	3.20	0.50	1.22	2.47

rate was kept constant during the sintering. The densities of the partially sintered substrates were calculated from the sintered weights and volumes. The densities of the fully sintered parts were measured using the Archimedes method.

2.2. Thermal conductivity measurement

The thermal conductivity was measured by the laser flash technique [14]. The sample was coated on both its faces with a thin layer of evaporated gold in order to prevent direct transmission of the laser beam through the sample. The entire sample surface was then coated with graphite to aid in both the absorptivity of the front surface, and the emissivity of the back surface. The transient temperature–time response of the back face was measured and analysed to give the value for the thermal diffusivity [15]. The time corresponding to one-half of this temperature rise was designated $t_{1/2}$.

The theoretical model [15] used to evaluate the thermal diffusivity assumes that the heat pulse is instantaneous. However, when the duration of the pulse is comparable to the characteristic rise time of the rear face temperature, the increase of that temperature is delayed. Since the $t_{1/2}$ for thin AlN is less than about 1.5 ms, the measurement of the temperature rise by the i.r. detector begins before the latter part of the laser pulse reaches the sample. Under these conditions, it is evident that the measurement has violated the boundary condition of the theoretical model. In order to take this effect into account, a finite pulse width correction as suggested by Taylor [16] was applied to the raw diffusivity data. From Taylor's function, the following correction equation was calculated:

$$\alpha_{corr} = \frac{0.333L^2}{2.402t_{1/2} - \tau}$$

where α_{corr} is the corrected thermal diffusivity ($cm^2\,s^{-1}$), L the thickness of the sample (cm), $t_{1/2}$ the half-rise time (ms) and $\tau = 0.350$ ms. The thermal conductivity K was determined as follows [16]:

$$K = 100\alpha_{corr}\rho C_p$$

where K is the thermal conductivity ($W\,m^{-1}\,K^{-1}$), ρ the density ($g\,cm^{-3}$) and $C_p = 0.738\,J\,g^{-1}\,K^{-1}$ is the heat capacity of AlN.

2.3. X-ray diffraction and electron microscopy

A Rigaku diffractometer using CuK_α radiation was used to generate a powder diffraction pattern over the required 2θ range at a scan rate of $5°\,min^{-1}$. Scanning electron microscopy (SEM) on both fractured and polished samples was performed. Specimens for transmission electron microscopy (TEM) were prepared using the standard procedures for ceramic materials. Discs, 3 mm in diameter and ~ 150 μm thickness, were ultrasonically cut from polished thin sections, and dimpled to a thickness of ~ 20 μm in the centre. These discs were then ion-beam-milled to perforation, and evaporation-coated with a thin layer of carbon. These specimens were examined by TEM (400T, Philips) operating at 120 keV. X-ray energy-dispersive spectroscopy (EDS) was also performed on these specimens during TEM.

3. Results and discussion

Fig. 1 shows the thermal conductivity as a function of sintering time at 1810 °C. The thermal conductivity shows a very strong dependence on the sintering time, in that the values increase monotonically from $138\,W\,m^{-1}\,K^{-1}$ (2 h) to $172\,W\,m^{-1}\,K^{-1}$ (8 h). The measured densities of the sintered samples varied from 3.28 to $3.30\,g\,cm^{-3}$ (theoretical density $\simeq 3.32\,g\,cm^{-3}$). Unfortunately, the Archimedes technique employed in this study was not sufficiently sensitive to detect any significant variation in the degree of porosity between the specimens. Accordingly, SEM examination was performed on both samples with high and low thermal conductivity, in order to determine possible microstructural differences which could account for the change in thermal properties. Fig. 2a and b are back-scattered electron micrographs showing the microstructures for the low thermal conductivity sample (LC, sintered for 2 h), and the high thermal conductivity sample (HC, sintered for 8 h), respectively. Clearly, the second phase is more uniformly dispersed in the HC sample. Furthermore, the HC sample contains less porosity relative to the LC sample. To further illustrate the difference, a fracture surface examination was performed on both the HC and LC samples using SEM. Fig. 3a shows the fracture surface of the LC sample. From this micrograph it can be seen that there is extensive porosity, and that in some areas there are excess amounts of grain boundary phase. By contrast, the fracture surface of the high thermal conductivity sample (Fig. 3b) shows a fully dense structure, with little evidence of a wetting second phase. Another interesting feature is that most of the AlN grains have a spherical shape morphology in the LC samples, whereas they exhibit a more well-defined hexagonal morphology in the HC sample.

A more detailed comparison of the morphology and distribution of second phase in the two types of specimen was carried out by TEM. Fig. 4 shows a representative TEM micrograph taken from the LC specimen. In general, for this specimen the grain boundary

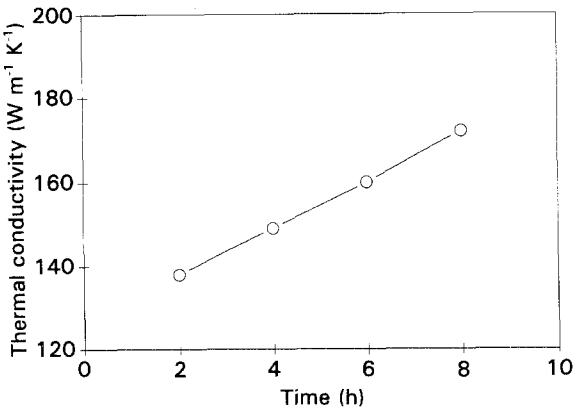

Figure 1 Thermal conductivity as a function of sintering time at 1810 °C.

phase was seen to penetrate along the grain boundaries, thus resulting in low values of the dihedral angle. Fig. 5 is a TEM micrograph showing the morphology and the location of the grain boundary phase for the HC specimen. In this case, the second phase consisted of small, discrete particles which were located mainly at grain triple points. For the particle shown in Fig. 5, the dihedral angle was estimated to be approximately 60°.

Fig. 6 shows a typical X-ray diffraction pattern for the sintered samples. As expected, the major crystalline phase was identified as AlN. However, additional peaks were obtained which could be consistently indexed as corresponding to yttrium aluminium garnet, $Y_3Al_5O_{12}$ (YAG). Further confirmation that the grain

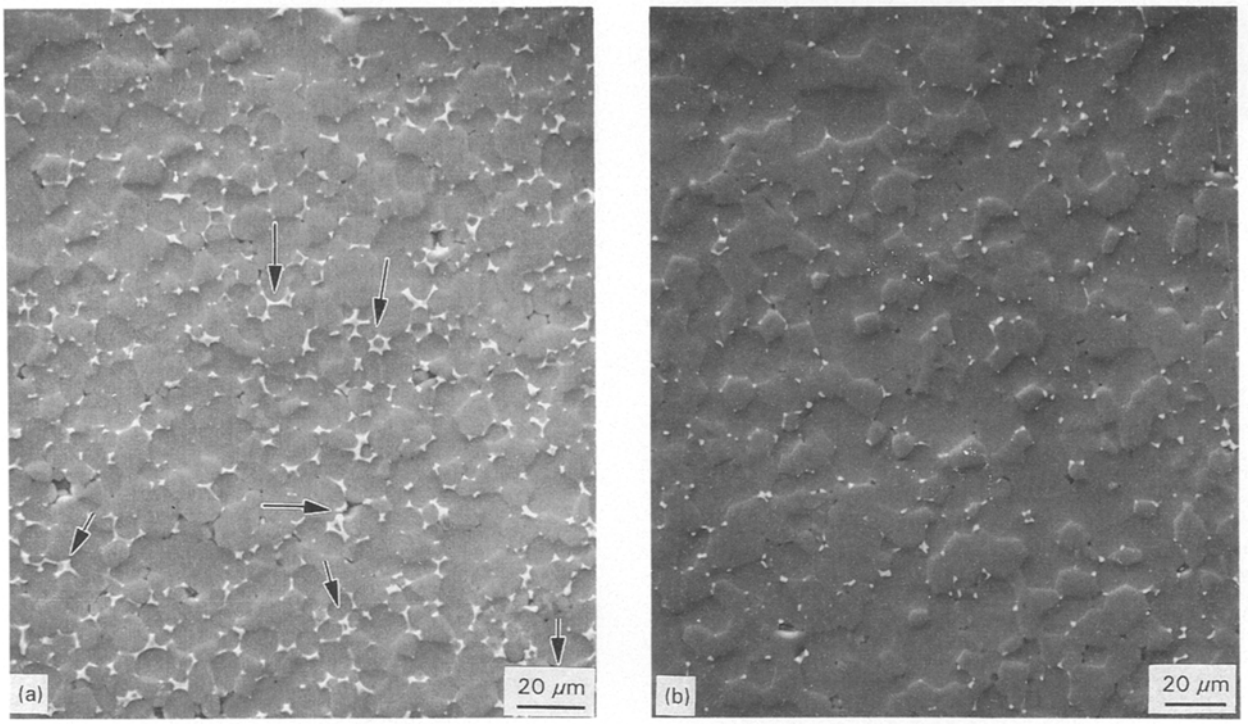

Figure 2 Back-scattered electron SEM micrograph showing the difference in the grain boundary phase distribution for samples sintered at 1810 °C for (a) 2 h (LC) and (b) 8 h (HC).

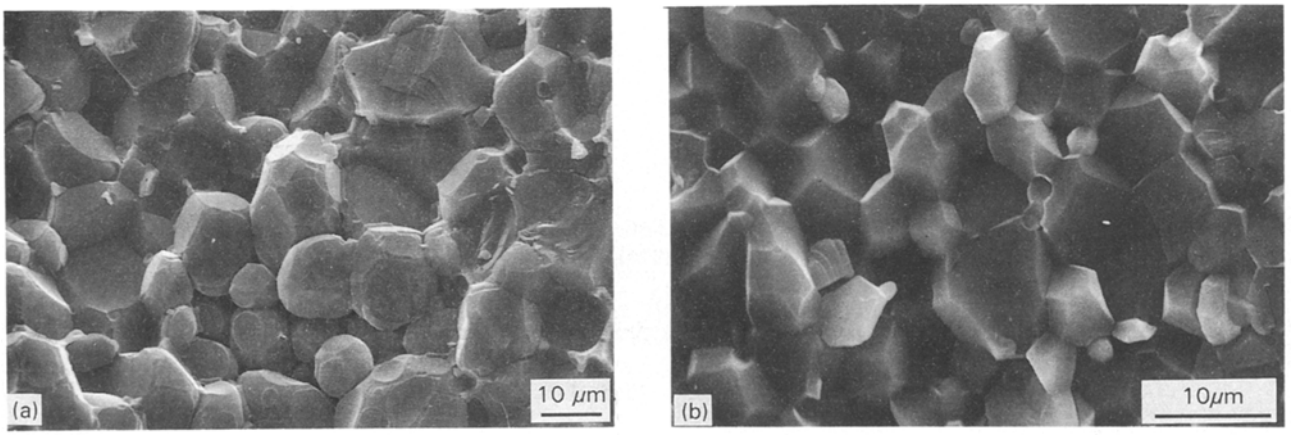

Figure 3 SEM micrograph taken from the fracture surface of sample sintered at 1810 °C for (a) 2 h (LC) and (b) 8 h (HC).

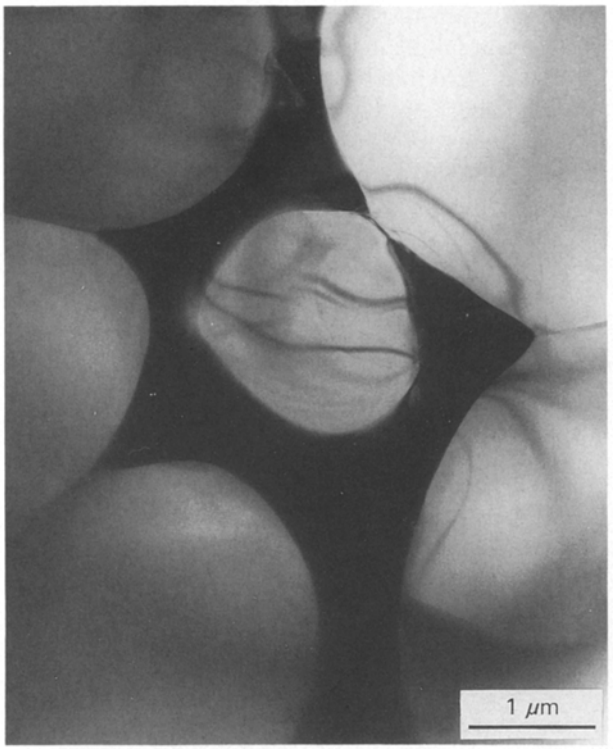

Figure 4 Bright-field TEM micrograph showing the morphology and location of the grain boundary phase from specimen LC sintered at 1810 °C for 2 h.

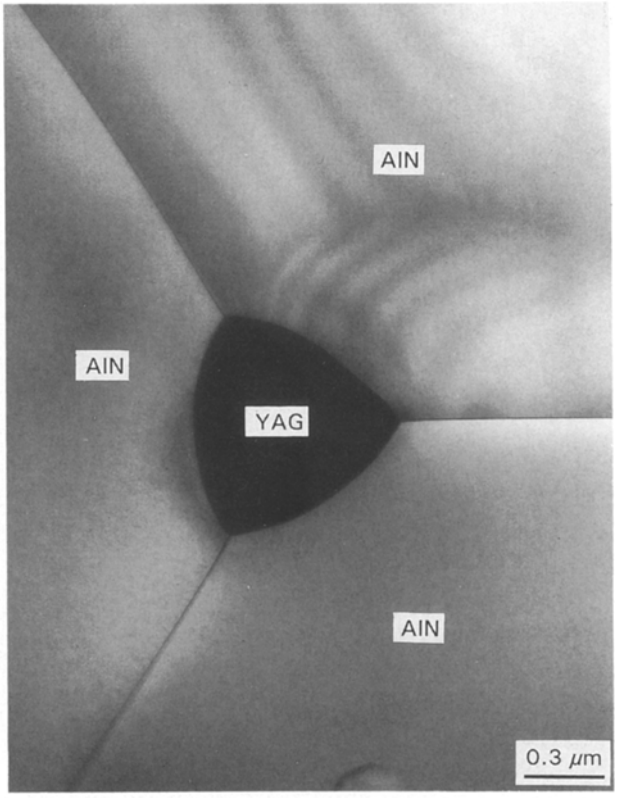

Figure 5 Bright-field TEM micrograph showing the morphology and location of the grain boundary phase from specimen HC sintered at 1810 °C for 8 h.

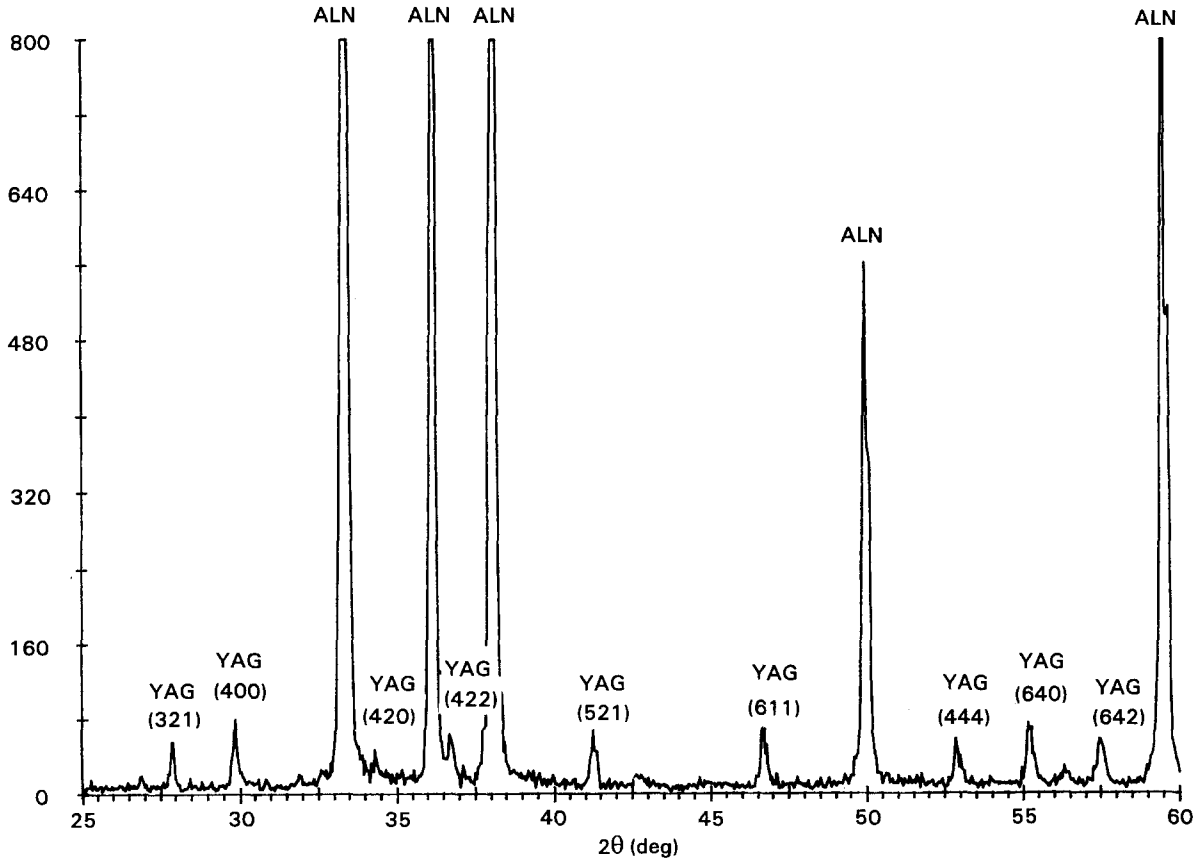

Figure 6 X-ray diffraction pattern showing AlN as the major crystalline phase, and $Y_3Al_5O_{12}$ (yttrium aluminium garnet) as the minor crystalline phase.

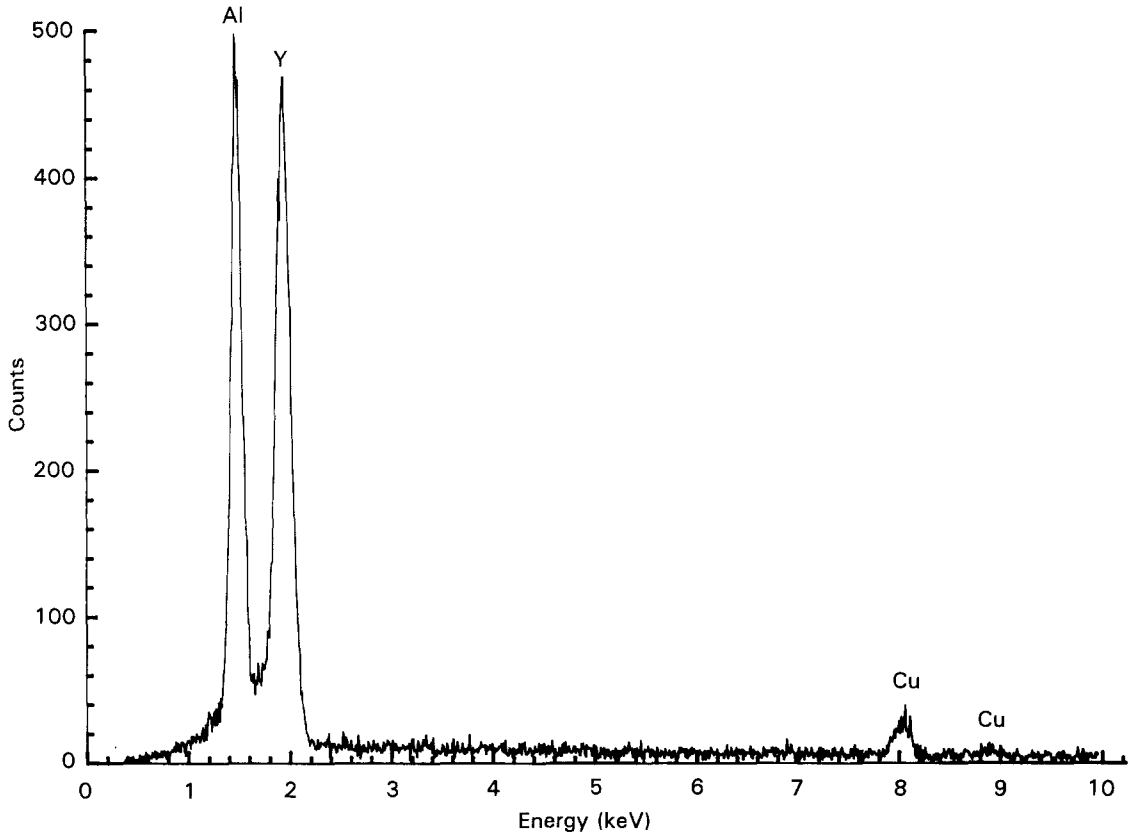

Figure 7 Energy-dispersive spectrum from the crystalline grain boundary phase (sample HC).

boundary second phase was indeed YAG was provided by both electron diffraction, and compositional analysis using EDS. A typical EDS spectrum obtained from a second-phase particle is shown in Fig. 7. Expressed in terms of a solid solution between alumina and yttria, the composition of the grain boundary phase was found to be $0.373Y_2O_3 \cdot 0.627Al_2O_3$, which is almost identical to the YAG composition $3Al_2O_3 \cdot 5Y_2O_3$. Within experimental scatter, no difference in second-phase composition was detected for the LC and HC samples.

The origin of the YAG second phase in the sintered AlN samples is postulated to be as follows. As can be seen from Table I, the AlN powder contains a significant amount of oxygen as an impurity element. It is believed that the oxygen is present in the form of a thin layer of aluminium oxide on the AlN powder surface, and that it reacts with Y_2O_3 to form a low melting-point eutectic phase. This phase is assumed to be liquid at the sintering temperature, and gives rise to crystalline YAG on solidification.

The influence of sintering time on the thermal conductivity may now be rationalized in the following manner. As mentioned earlier, in non-metallic solids heat is conducted mainly by phonons. Since porosity can significantly increase the degree of phonon scattering, it is perhaps not surprising that the sample sintered for the shortest time, and possessing the highest porosity, exhibited the lowest thermal conductivity. The high porosity of the LC sample is believed to be closely related to the non-uniform distribution of second phase. As the sintering time is increased, however, the liquid phase becomes more uniformly distributed through the structure. The resultant improvement in the thermal conductivity is believed to arise from a combination of the lower porosity, and the fact that the second phase is now non-wetting, and confined to the triple points.

Finally, some comment concerning the observed change in dihedral angle is perhaps warranted. Given that no compositional difference was detected, the change in the wetting characteristics is difficult to rationalize. It seems feasible, however, that the explanation lies in very small changes in the chemistry of the liquid phase and particle/grain surfaces, which take place during the sintering process.

4. Summary

Using a fine AlN powder of high purity, polycrystalline AlN ceramics with thermal conductivity greater than 170 $W m^{-1} K^{-1}$ were processed. All the sintered samples contained YAG as a second phase, which is believed to have been formed by reaction of Y_2O_3 (added as a sintering aid) with oxygen impurity present as Al_2O_3. As the sintering time increased, it was observed that the second phase became less wetting, and also its distribution became more uniform. At the same time, the degree of porosity in the samples was significantly reduced. The improvement in thermal conductivity with sintering time can thus be attributed to a combination of the aforementioned microstructural changes.

References

1. N. KURAMOTO and H. TANIGUCHI, *J. Mater. Sci. Lett.* **3** (1984) 471.

2. W. WERDECKER and F. ALDINGER, *IEEE Trans. Compon. Hybrids Manuf. Technol.* **CHMT-7** (4) (1984) 399.
3. C.-F. CHEN, in Proceedings of IEPS 9th Annual International Electronic Package Conference, San Diego, 1989 (The American Ceramic Soc., Westerville, OH) p. 1291.
4. M. P. BOROM, G. A. SLACK and J. W. SZYMASZEK, *Amer. Ceram. Bull.* **51** (1972) 852.
5. G. A. SLACK, *J. Phys. Chem. Solids* **34** (1973) 321.
6. G. A. SLACK, R. A. TANZILLI, R. O. POHL and J. W. VANDERSANDE, *ibid.* **48** (1987) 641.
7. N. KURAMOTO, H. TANIGUCHI and I. ASO, *IEEE Trans. Compon. Hybrids Manuf. Techol.* **9** (1986) 386.
8. *Idem, Amer. Ceram. Bull.* **68** (1989) 883.
9. Y. KUROKAWA, K. UTSUMI and H. TAKAMIZAWA, *J. Amer. Ceram. Soc.* **71** (1988) 588.
10. M. F. DENANOT and J. RABIER, *J. Mater. Sci.* **24** (1989) 1594.
11. L. WEISENBACH, J. A. S. IKEDA and Y.-M. CHIANG, in "Ceramic Substrates and Packages for Electronic Applications", Advances in Ceramics Vol. 26, edited by M. F. Yan, H. M. O'Bryan Jr, K. Niwa and W. S. Young, p. 133.
12. A. V. VIRKAR, T. B. JACKSON and R. A. CUTLER, *J. Amer. Ceram. Soc.* **72** (1989) 2031.
13. C.-F. CHEN and E. SAVRUN, in "Materials and Processes for Microelectronic Systems", Ceramic Transactions Vol. 15, edited by K. M. Nair, R. Pohanka and R. C. Buchanan (The American Ceramic Soc., Westerville, OH, 1991) p. 193.
14. D. P. H. HASSELMAN and G. A. MERKEL, *J. Amer. Ceram. Soc.* **72** (1989) 967.
15. W. J. PARKER, R. J. JENKINS, C. P. BUTLER and G. L. ABBOTT, *J. Appl. Phys.* **32** (1961) 1679.
16. R. E. TAYLOR, Report PB-225 591 (NTIS, US Department of Commerce, Springfield, VA, 1973).

Received 5 January
and accepted 1 September 1993